Simulative Investigation of Transfer Function-based Disturbance Observer for Disturbance Estimation on Electromechanical Axes

Chris Schöberlein[1], Armin Schleinitz[1], Holger Schlegel[1] and Matthias Putz[1,2]
[1]*Institute of Machine Tools and Production Processes, Chemnitz University of Technology, Reichenhainer Straße 70, 09126 Chemnitz, Germany*
[2]*Fraunhofer-Institut for Machine Tools and Forming Technologies, Reichenhainer Straße 70, 09126 Chemnitz, Germany*

Keywords: Electromechanical Axes, Disturbance Estimation, Process Forces, Transfer Function, Simulation Model, Frequency Response.

Abstract: In the field of machine tools, applicable solutions for monitoring process forces are becoming increasingly important. In addition to sensor-based approaches there are also methods which utilize the already available signals of the machine control. Usually, the motor currents and, when applicable, position values of the feed axes are considered. By applying reduced order models of the machine axes, non-process components are subtracted from the measured signals. However, these approaches are often utilizing simplified models or require additional a-priori knowledge, for example construction data or actual parameter values. The former in particular has a negative impact on the quality of the estimations. To overcome these disadvantages, this paper presents a novel observer structure based on the mechanical system transfer function of the feed axis. One main advantage is achieved by applying scalable and automatically generated models with focus on distinct frequency ranges. All necessary information is provided by a frequency response of the speed control plant, as it is typically obtained during the commissioning phase of electromechanical feed axes. By inverting the system transfer function and considering an additional disturbance transfer function, the quality of the estimation can be significantly improved compared to previous approaches.

SCITEPRESS SCIENCE AND TECHNOLOGY PUBLICATIONS

1 INTRODUCTION

The measurement of the forces acting during manufacturing processes is subject of intensive research efforts. In industrial application, additional sensors are commonly utilized and placed close to the contact point between tool and workpiece. Due to its proximity to the process, these methods are characterized by a high sensitivity, but at the same time increase the complexity of the machine and lead to additional investment costs (Rizal et al., 2014).

For this reason, there are in particular research-based approaches which aim to reconstruct the prevailing process forces from the already available signals of the installed drive components. The majority of these approaches focusses on the pure evaluation of the motor currents of the feed axes (Stein & Shin, 1986; Altintas, 1992; Sato et al., 2013). An alternative is provided by so-called disturbance observers. These consist usually of an order-reduced model of the mechanical system of the axes and utilize additional speed and position values. An overview of the basic methods and its characteristics as well as a simulative comparison is presented in (Schöberlein et al., 2020).

All these methods have in common that simplified models and deviations in the system parameters affect the accuracy of the estimation. However, the estimation quality can be improved for individual approaches. (Yamato et al., 2019) takes the position dependency of certain system variables into account and (Yamada et al., 2016) separates individual vibration components, for example. On the other hand, these methods are often only applicable in certain frequency ranges and typically require detailed system knowledge. Within the scope of this paper, a novel approach will be presented, which is based solely on drive-internal measurement functions. As a consequence of the applied model generation method, no prior system knowledge is required.

The paper has the following structure. Section 2 describes the structure of a typical machine tool axis as well as approaches for modelling its mechanical

Schöberlein, C., Schleinitz, A., Schlegel, H. and Putz, M.
Simulative Investigation of Transfer Function-based Disturbance Observer for Disturbance Estimation on Electromechanical Axes.
DOI: 10.5220/0009858606510658
In *Proceedings of the 17th International Conference on Informatics in Control, Automation and Robotics (ICINCO 2020)*, pages 651-658
ISBN: 978-989-758-442-8
Copyright © 2020 by SCITEPRESS – Science and Technology Publications, Lda. All rights reserved

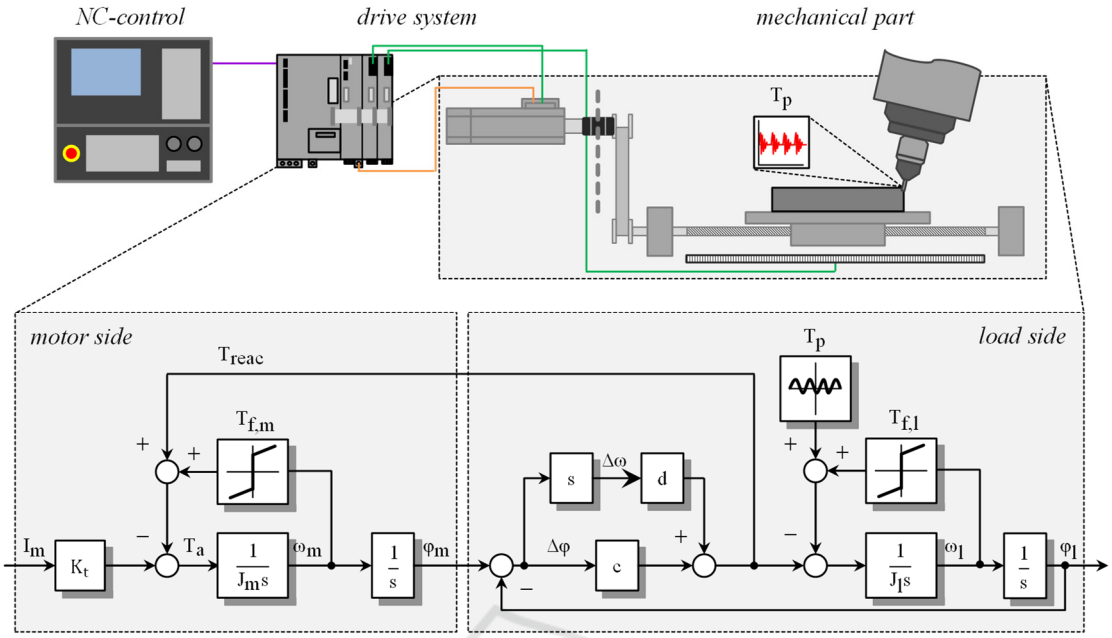

Figure 1: Structure of the electromechanical axis and block diagram of the mechanical two-mass system.

transfer behaviour. Moreover, a method is presented which generates scalable models of the mechanical system transfer function based on frequency response measurements of the speed control plant.

In order to enhance the estimation accuracy for load-side disturbances, an additional disturbance transfer function is introduced. Section 3 is focussed on the actual observer structure of the novel transfer function disturbance observer (TFDOB). For this purpose, two concepts for inverting the previously determined transfer functions are presented. One approach is based on the extension of the transfer function by an additional P-controller. The other one focusses on the placement of additional high-frequency poles. In Section 4, the TFDOB is implemented in a simulation model in Matlab® Simulink® and compared with a common observer structure. The paper closes with a summary and an outlook on upcoming research goals.

2 AUTOMATIC MODELLING OF MECHANICAL TRANSFER FUNCTION

The typical structure of an electromechanical feed axis is shown in Figure 1. Usually, it can be separated into an electrical part consisting of an NC control and a subordinated drive system as well as a mechanical part. In most applications, the mechanical system is realized in form of a ball screw drive. As illustrated in the Figure, process forces usually act on the load side of the mechanical part only. Position measuring systems are equipped on motor and load side, respectively. For reasons of simplification, a rotary system is assumed for the following investigations. Hence, the equilibrium of torques is calculated to:

$$T_m = I_m \cdot K_t = T_a + T_l \quad (1)$$

T_m identifies the motor torque provided by the motor, which is calculated as product of motor current I_m and torque constant K_t. The parameter T_a denotes the acceleration torque required for the movement of the axis and T_l summarizes all load torques acting on the motor:

$$T_l = T_p + T_f + T_g \quad (2)$$

As shown in equation (2), besides friction (T_f) and potential weight torques (T_g) the process torques T_p are included in the load torque and therefore also affect the actual motor torque.

2.1 Modelling of Electromechanical Axes

Modelling strategies for electromechanical axes usually concentrate solely on the mechanical part. Typically, this part is represented in form of a multi-

mass mechanism. Depending on the complexity and modelling accuracy, more or less complex models can be applied. A widely utilized model in control engineering is the two-mass system (Figure 1, lower part), which is selected for the following considerations. Such a system is typically divided into the following components:

- motor-side moment of inertia J_m,
- load-side moment of inertia J_l,
- elastic coupling between J_m and J_l with the torsional rigidity c and damping constant d.

Additional friction torques act on motor ($T_{f,m}$) and load side ($T_{f,l}$), respectively. Process forces usually act on the load side only. The total moment of inertia for a general multi-mass system is calculated as follows:

$$J_{tot}=\sum_{i=1}^{n} J_i \tag{3}$$

With reference to formula (3), the following transfer function results for a two-mass system:

$$G_{S,2MS}(s)=\frac{1}{J_{tot}\cdot s}\cdot\frac{\frac{J_l}{d}\cdot s^2+\frac{d}{c}\cdot s+1}{\frac{J_m J_l}{J_{tot} c}\cdot s^2+\frac{d}{c}\cdot s+1} \tag{4}$$

In principle, higher-order models can also be described with physical parameters. On the other hand, for systems with model orders higher than three this is no longer feasible with reasonable effort (Münster et al., 2014). In addition to the representation with physical parameters shown in formula (4), the two-mass system can also be described with standardized parameters (Hipp et al, 2017):

$$G_{S,2MS}(s)=\frac{1}{J_{tot}\cdot s}\cdot\frac{\left(\frac{1}{\omega_f}\right)^2\cdot s^2+\frac{2d_f}{\omega_f}\cdot s+1}{\left(\frac{1}{\omega_r}\right)^2\cdot s^2+\frac{2d_r}{\omega_r}\cdot s+1} \tag{5}$$

Here ω_r and ω_f denote the resonance and antiresonance frequencies, d_r and d_f the associated damping values. As shown in Figure 2, ω_r and ω_f can be taken directly from the frequency response of the mechanical system. The damping values can only be identified with great effort. Hence, they are often determined empirically or utilizing heuristic methods (Hipp et al., 2017).

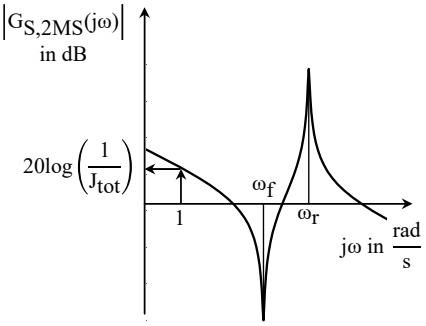

Figure 2: Magnitude response of a two-mass system.

2.2 Automatic Model Generation based on Frequency Measurements

In order to implement the novel TFDOB, the transfer function of the mechanical system is required. As illustrated in formula (5), it can be represented by standardized parameters. A method to generate these transfer functions automatically is proposed in (Münster et al., 2014) and (Hipp et al., 2017). This methodology can be applied to systems of arbitrary order. The starting point is a measured frequency response of the mechanical subsystem of the feed axis. Modern control and drive systems offer corresponding pre-installed functionalities. The frequency response is emulated by connecting individual partial oscillators in series. Each partial oscillator represents a characteristic part of the frequency response in the direct and indirect case (Figure 3). The resulting transfer function of such a

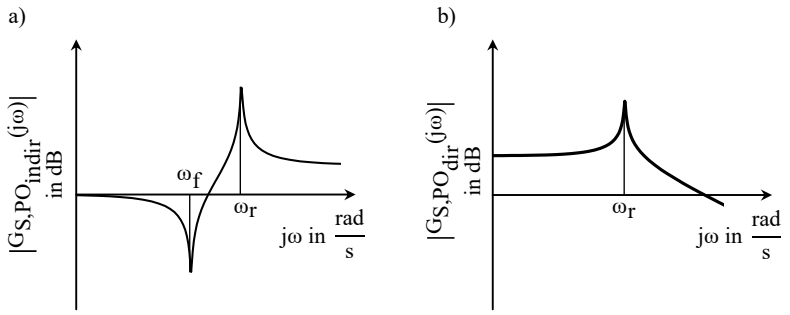

Figure 3: Partial oscillator for indirect (a) and direct (b) controlled systems.

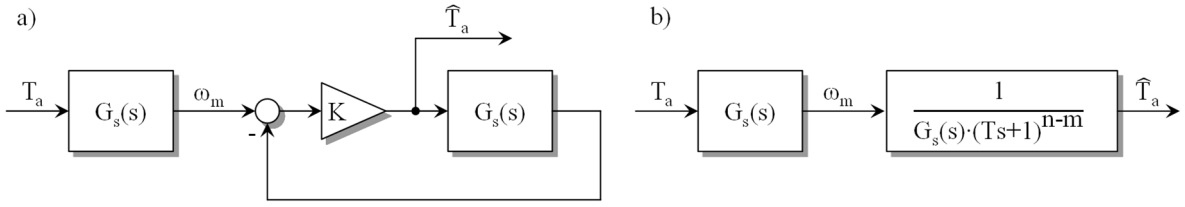

Figure 4: Block diagram of the transfer function inverter with proportional gain (a) and pole placement (b).

partial oscillator is calculated as:

$$G_{S,PO}(s)=\frac{a\cdot\left(\frac{1}{\omega_f}\right)^2\cdot s^2+\frac{2d_f}{\omega_f}\cdot s+1}{\left(\frac{1}{\omega_r}\right)^2\cdot s^2+\frac{2d_r}{\omega_r}\cdot s+1} \quad (6)$$

Note that for indirect controlled systems the parameter a is assigned with 1 and for direct controlled systems a is 0. The general procedure for a measured frequency response according to (Hipp et al., 2017) is:

1. determination of J_{tot} by calculating the gradient at lower frequencies,
2. identification of the resonance and anti-resonance frequencies,
3. initialization of the damping parameters with default value of 0.01,
4. empirical adaptation of the damping values.

The fundamental suitability of the proposed method is demonstrated on an exemplary simulated frequency response model in Section 4.

3 TRANSFER FUNCTION BASED DISTURBANCE OBSERVER

The following Section presents a novel type of disturbance observer based on automatic generated transfer functions. One main advantage of this method is that a detailed and scalable model of the mechanical transfer behaviour is created even without complex reference measurements, like applied in (Rudolf, 2014). Since the process forces usually act on the load side of the feed axis, an additional disturbance transfer function is introduced. Therefore, no further measurements or system knowledge are required.

3.1 Inversion of Mechanical System Transfer Function

The fundamental idea of model-based approaches for estimating process forces on feed axes is based on the assumption that these forces are contained in the motor current signal. As a consequence, the process forces can be reconstructed by subtracting all non-process influences (e.g. friction, acceleration). As a result of the knowledge of the mechanical transfer behaviour, the torque required for axis acceleration can be obtained. Due to the fact that the actual angular velocity is typically available in modern drive systems, this acceleration torque is calculated by inverting the mechanical transfer function $G_s(s)$:

$$G_S(s)=\frac{\omega_m(s)}{T_a(s)}=\frac{N(s)}{D(s)}\rightarrow G_S(s)^{-1}=\frac{D(s)}{N(s)} \quad (7)$$

As a result of the inversion, the poles of the original system become the zeros of the inverted system and vice versa. If this inversion is carried out using the exemplary transfer function of the two-mass system from equation (5), the inverted system would have a differentiating character. This means that the order of the numerator N(s) is greater than the order of the denominator D(s). However, such a system cannot be implemented in reality for reasons of causality (Schröder, 2015). Hence, two alternative concepts for inverting the transfer function are considered (Buchholz, 2007), both illustrated as block diagram in Figure 4. In the left part of the illustration (a), the inversion is realized by inserting the original transfer function into the feedback path of a P-controller with high controller gain K. This leads to the following transfer function:

$$G_S(s)^{-1}=\frac{T_a(s)}{\omega_m(s)}=\frac{D(s)}{N(s)}=\frac{K}{1+K\cdot G_S(s)} \quad (8)$$

$$G_S(s)^{-1}=\frac{K}{1+K\cdot\frac{N(s)}{D(s)}}=\frac{K\cdot D(s)}{D(s)+K\cdot N(s)} \quad (9)$$

It becomes clear that the zeros of the inverted function, depending on the value of K, correspond to the poles of the original transfer function. The poles of the inverted function are equally dependent on K, whereby for large values of K:

$$\lim_{K\rightarrow\infty} G_S(s)^{-1}=\frac{D(s)}{N(s)} \quad (10)$$

For continuous systems, this method delivers very good results depending on the value of the controller gain and an appropriate selection of the solver type (e.g. ode15s) in Matlab® Simulink®. For practical systems with discrete input signals, however, the necessary high gain factors lead to discontinuities and a truncation of the simulation. In consequence, this structure is unsuitable for the intended application in discrete controlled drive systems. Hence, a second concept is proposed, which is shown in Figure 4b. The fundamental idea here is to extend the inverted transfer function with a defined number of high-frequency poles until the denominator order corresponds at least to the numerator order:

$$G_S(s)^{-1}=\frac{T_a(s)}{\omega_m(s)}=G_S(s)^{-1}\cdot\frac{1}{(1+Ts)^{n-m}} \tag{11}$$

Main advantage of this inverter structure is its robustness regarding digital systems and signals. Hence, this approach will be utilized in the following and examined in detail in Section 4 for an exemplary simulated mechanical system.

3.2 Load Disturbance Transfer Function

As already explained, the process forces usually act on the load side of the feed axis. Depending on the type of the mechanical subsystem, the knowledge of the transfer behaviour between the surgical point of the disturbance torque T_p and the reaction torque T_{reac} on the motor side may lead to further improvements of the estimation. The parameters of this transfer function can be obtained once more from the mechanical frequency response. In general case, the transfer function results to:

$$G_{dist}(s)=\frac{T_{reac}}{T_p}=\prod_{i=1}^{n}\frac{s^2+\frac{2d_{f,i}}{\omega_{f,i}}\cdot s+1}{\left(\frac{1}{\omega_{f,i}}\right)^2\cdot s^2+\frac{2d_{f,i}}{\omega_{f,i}}\cdot s+1} \tag{12}$$

Again, this transfer function is inverted according to the previously described strategy by adding high-frequency poles. The combination of both systems leads to the observer structure shown in Figure 5. Note that due to the intended application on digital systems, the transfer functions are transformed into z-domain. Furthermore, besides acceleration and disturbance torques an additional friction model is required. This paper does not provide a detailed description of possible friction models. For example, an approach consisting of four individual friction parts is discussed in (Schöberlein et al., 2020).

4 SIMULATION RESULTS

In this Section, the TFDOB is verified based on simulations in Matlab® Simulink®. Hence, a second-order system with the parameters listed in table 1 is utilized as representative mechanical model and implemented as block simulation (see Figure 1). The cycle time of the observer and its input signals is set to a typical value of 100 µs. As described in (Schöberlein et al., 2020), the current control loop was approximated as a PT2 element. Furthermore, a current setpoint filter to attenuate the resonance frequency as well as a low-pass filter with a cut-off frequency of 1999 Hz were implemented. The speed controller was parameterized corresponding to the setting rule of the symmetrical optimum. All parameters are listed in table 2.

4.1 Inversion of System Transfer Function

First, the inverted transfer functions of the mechanical system for acceleration and disturbance torque are calculated. Hence, the measured frequency response is analyzed by utilizing the methodology described in Section 2.2. The results are illustrated in Figures 6 and 7. Figure 6a shows the result of the frequency response estimation in the Bode diagram. All identified parameters are listed in Table 1.

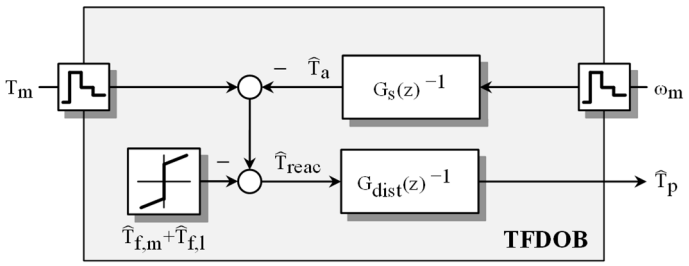

Figure 5: Block diagram of the complete TFDOB.

Table 1: Parameters of the simulated two-mass system.

System parameters		Identified parameters	
J_{tot} (kg·m^2)	0.001354	J_{tot} (kg·m^2)	0.00137
J_m (kg·m^2)	0.000869	ω_f (Hz)	334.00
J_l (kg·m^2)	0.000485	d_f	0.040
$c_{m,l}$ $\left(\frac{Nm}{rad}\right)$	2150	ω_r (Hz)	423.19
$d_{m,l}$ $\left(\frac{Nms}{rad}\right)$	0.086	d_r	0.055

Table 2: Speed controller settings.

Speed controller			
K_p $(\frac{Nms}{rad})$	0.0802		
T_n (s)	0.00842		
T_{SSPF} (s)	0.002		
Current setpoint filter			
ω_{FCN} (Hz)	418.18 1999.00	ω_{FCD} (Hz)	418.18 1999.00
D_{FCN}	0.0 0.7	D_{FCD}	0.25 0.7

It can be stated that despite small deviations for the estimated value of J_{tot}, the approximated model emulates the block simulation very well. The adjusted damping values for the green colored model were determined empirically. Compared to the red colored model with default damping values, a significant improved approximation quality of the original model is achieved. Figure 7a shows the pole-zero map for the estimated discrete transfer function and its inversion for different values of the time constant T. Regardless of the time constant T, the pole and zero positions of the transfer function are reproduced very precisely. Furthermore, all poles of the inverted transfer function are placed within the unit circle around the origin of coordinates. This means that the inverted system is stable. The essential effect of smaller time constants is expressed in the position of the additional real poles, which influences the bandwidth of the estimation.

4.2 Inversion of Load Disturbance Transfer Function

In addition to the inverted transfer function of the mechanical subsystem, the TFDOB includes the transfer behaviour for load-side disturbances defined in Section 3.2. Figure 6b shows the Bode diagram for the block simulation and the approximated transfer behaviour for default and adjusted damping values based on equation (11). Once again, there is good agreement between simulated and identified transfer behaviour especially for the adapted damping values. Considering the pole-zero map in Figure 7b for the inverted discrete disturbance transfer function for various time constants, the results of the mechanical transfer function can be confirmed. This inverted transfer function is stable, too. Furthermore, the additional real poles again are shifting in the negative direction for smaller time constants T.

4.3 Approximation of Disturbance Torques

After the functionality of the individual subsystems has been verified, the complete TFDOB is set up according to Figure 5. To evaluate its performance, the estimation behaviour in time and frequency

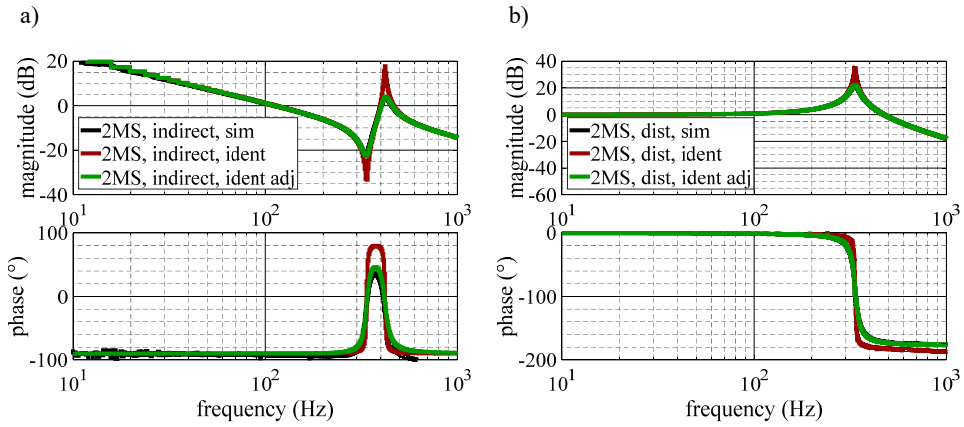

Figure 6: Frequency response for simulated and identified system (a) and disturbance transfer function (b).

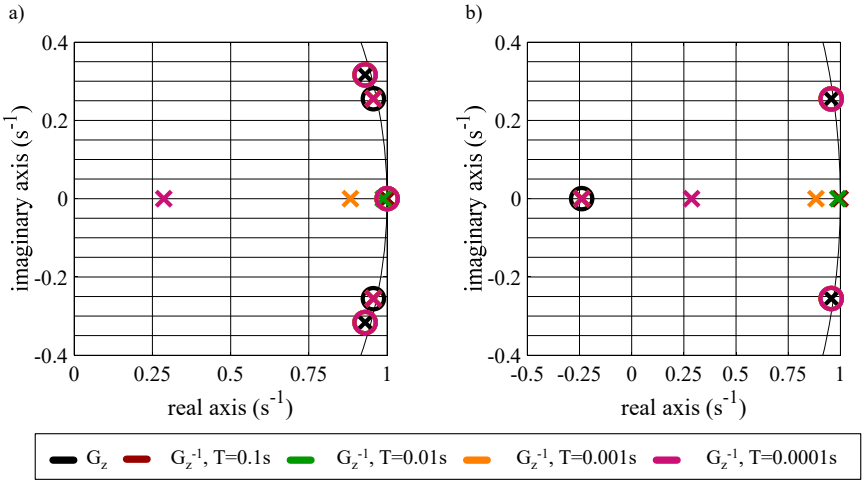

Figure 7: Pole-zero-map for simulated and inverted system (a) and disturbance transfer function (b).

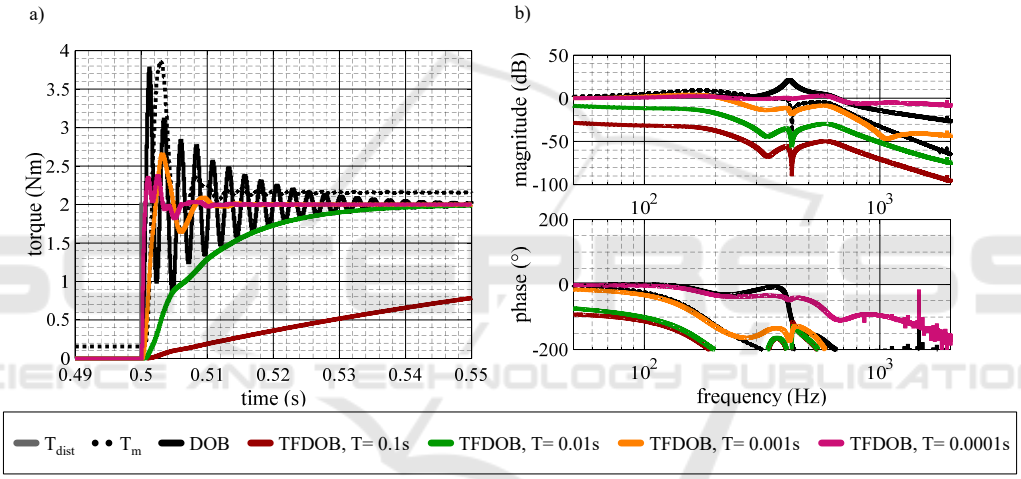

Figure 8: Simulated step (a) and frequency (b) response for load side disturbance torque.

domain is examined. Hence, a stepwise and broadband disturbance excitation is applied, respectively. The disturbance input is connected to the load side with a magnitude of 2 Nm. To avoid static friction effects, a speed offset of 50 min^{-1} was specified. The additional time constants of the inverted transfer functions of the TFDOB were gradually decreased from 0.1 s to 100 µs. For reasons of comparison, the conventional disturbance observer (DOB) is included in the simulation, too. This observer is also based on measurements of the motor current and speed. Its only free parameter is the total moment of inertia, which has been assigned with the estimated value (see Table 1). Furthermore, a pure evaluation of the motor current or rather the motor torque was taken into account. The simulated friction behaviour corresponds to the parameterization in (Schöberlein et al., 2020). For the stepwise disturbance input in time domain (Figure 8a), in contrast to the DOB, an excitation of the mechanical natural frequency is avoided for all parameterizations of the TFDOB. On the other hand, the dimension of the time constant significantly affects the dynamics of the estimation. It should be selected as small as possible, whereby modern drive systems with higher clock rates may grant further improvements. In contrast to a pure evaluation of the motor current, the estimation dynamics of the TFDOB and DOB are significantly increased.The results can also be confirmed for a broadband disturbance excitation in frequency domain, whereby the visible influence of the current setpoint filter is counteracted for smaller time constants of the TFDOB. Overall, the estimation behaviour compared to the DOB or a pure motor current evaluation is significantly improved over a wide frequency range. This effect should become

significant for more complex mechanical systems, for example with lower natural frequencies or further partial oscillators. Due to the scalability of the presented identification and modelling approach, an increased estimation quality is expected even for elastically coupled multi-mass systems.

5 CONCLUSIONS

In this paper, the performance of a novel type of disturbance observer for electromechanical axes was examined using a simulation model in Matlab® Simulink®. The main advantages in contrast to established structures are the automatic identification of the observer parameters and their scalability on systems of multiple order. The determination of the required transfer functions is based exclusively on frequency response measurements. By inverting the determined transfer functions via additional high-frequency poles the estimation of load-side disturbances is enabled over a wide frequency range. The performance compared to an established structure was demonstrated utilizing an exemplary simulated electromechanical axis.

Future work should initially analyze the robustness of the observer structure. For example, this includes currently not considered influencing factors, such as signal noise or changing mechanical parameters and controller settings. A more precise identification of the damping values of the transfer functions, for example with heuristic optimization methods, may lead to further improvements. Finally, the TFDOB must be subjected to practical measurements on a real machine tool under process conditions. Hence, it should be examined if the novel structure can be supplemented by including signals of a load-side measuring system.

ACKNOWLEDGEMENTS

Funded by the European Union (European Social Fund) and the Free State of Saxony.

REFERENCES

Rizal, M., Ghani, J., Nuawi, M., Haron, C., 2014. Measurement of cutting forces in CNC turning centers: a review. In *International Journal of Mechanical Engineering, 7(10), 2083-2097*

Stein, J., Shin, K. 1986. Current monitoring of controlled DC spindle drives, In *Journal of Dynamic Systems, Measurement and Control, 108, 189-295*

Altintas, Y., 1992. Prediction of cutting forces and tool breakage in milling from feed drive current measurements. In *Journal of Engineering for Industry, 114, 386-392*

Sato, R., Hasegawa, M., Shirase, K., 2013. Cutting force monitoring based on the frequency analysis of feed motor torques. In *Journal of ME Japan*

Schöberlein, C., Norberger, M., Schlegel, H., Putz, M., 2020. Simulation and disturbance estimation of speed-controlled mechatronic drive systems. In *MATEC Web of Conferences, 306*

Yamato, S., Sugiyama, A., Suzuki, N., Irino, N., Imabeppu, Y., 2019. Enhancement of cutting force observer by identification of position and force-amplitude dependent model parameters. In *International Journal of Advanced Manufacturing Technology, 104, 3589-3605*

Yamada, S., Kakinuma, Y., 2016. Mode decoupled cutting force monitoring by applying multi encoder-based disturbance observer. In *International Journal on Advanced Manufacturing Technologies, 92, 4081-4093*

Münster, R., Walther, M., Schlegel, H., Drossel, W., 2014. Experimental and simulation-based investigation of a velocity controller extension on a ball screw system. In *Mechatronics 2014 – the 14th Mechatronics Forum International Conference, 226-234*

Hipp, K., Schöberlein, C., Schlegel, H., Neugebauer, R., 2017. Simulation based optimization for controller parametrization of machine tool axes – advanced application. In *Journal of Machine Engineering, 17(1), 57-68*

Rudolf, T. 2014. Adaptierbare Parametrierung von Diagnosesystemen durch Verwendung digitaler Antriebssignale in der Prozessüberwachung. In *Ergebnisse aus der Produktionstechnik*

Schröder, D. 2015. Elektrische Antriebe – Regelung von Antriebssystemen, Springer Vieweg. Heidelberg, 4th edition.

Buchholz, J. 2007. Inversion impossible? GRIN. Munich.